COMMUNICATION

Check for updates

Topochemical nitridation of Sr$_2$FeMoO$_6$†

Roberta Ceravola, [ID] [a] Carlos Frontera,[a] Judith Oró-Solé, [ID] [a] Ashley P. Black, [ID] [a] Clemens Ritter,[b] Ignasi Mata, [ID] [ac] Elies Molins, [ID] [a] Josep Fontcuberta [ID] *[a] and Amparo Fuertes [ID] *[a]

The topotactic nitridation of cation ordered, tetragonal Sr$_2$FeMoO$_6$ in NH$_3$ at moderate temperatures leads to cubic, $Fm\bar{3}m$ double perovskite oxynitride Sr$_2$FeMoO$_{4.9}$N$_{1.1}$ where double-exchange interactions determine ferromagnetic order with $T_C \approx$ 100 K. Substitution of oxide by nitride induces bond asymmetries and local electronically driven structural distortions, which combined with Fermi level lowering restricts charge itinerancy to confined regions and preclude spontaneous long-range magnetic order. Under a magnetic field, ferromagnetic correlations expand, favoring charge delocalization and a negative magnetoresistance is observed.

The introduction of nitride in oxidic compounds induces changes in the covalency of bonds, oxidation states of metals and energies of electronic levels; hence being a useful tool for the design of new materials.[1–4] Using this strategy transition metal perovskite oxynitrides[5] have been investigated in the last few years resulting in notable applications such as inorganic pigments,[6] visible light active photocatalysts,[7] and dielectric[8] and magnetic materials.[9]

Double perovskite oxynitrides A$_2$B′B″O$_{6-x}$N$_x$ (B = transition metal) are scarcely investigated although they potentially offer the possibilities of finding new properties by combining two different metals in the B sites. Cation order in double perovskites is a determining factor for physical properties and strongly affects the electronic and magnetic interactions between the two transition metals.[10] The synthesis of cation ordered double perovskite oxynitrides is not straightforward because high temperatures are needed to promote cation ordering, and under these conditions the oxynitrides may decompose into the more stable ternary or quaternary oxides.[11] On the other hand, solid state reactions at

lower temperatures under NH$_3$ between oxides or carbonates lead to disordered compounds. For instance LaMg$_{1/3}$Ta$_{2/3}$O$_2$N[12,13] or Sr$_2$FeMoO$_{6-x}$N$_x$[14] when prepared from mixtures of binary or ternary reactants under NH$_3$ at moderate temperatures shows a high degree of cation disorder. We have recently demonstrated that ammonolysis of cation ordered double perovskite oxides at low temperatures is a useful synthetic approach of the corresponding oxynitrides as it minimizes the mobility of the cations keeping the order of the precursor oxide.[15]

The double perovskite Sr$_2$FeMoO$_6$ (SFMO) is a singular material because it shows metallic conductivity, ferromagnetism (FM) above room temperature and a large negative magnetoresistance. These properties arise basically from the existence of a Fe-3d$^{6-\delta}$–Mo-(4d,5s)$^{\delta}$ mixed electronic configuration that gives rise to a broad, partially occupied conduction band which is fully spin polarized, as illustrated in Fig. 1a and b.[16,17] At room temperature
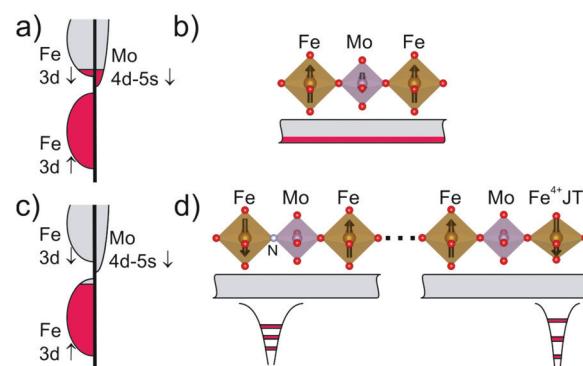

Fig. 1 (a) Schematic band filling of Sr$_2$FeMoO$_6$. The Fermi level is nearby the bottom of Fe-3dt$_{2g}$↓–Mo-(4d,5s)↓ bands. (b) In the oxide FeO$_6$ and MoO$_6$ octahedra are regular (top sketch) and the free carriers in the conduction band (bottom sketch) promote long range ferromagnetic order. (c) Schematic band filling of Sr$_2$FeMoO$_{4.9}$N$_{1.1}$. The oxidation of cations induced by N reduces the total number of electrons, and the filling of the bands. In the nitrided sample, the Fermi level shifts down to the top of the Fe-3d↑ band. (d) Localized states formed around defect-related potential wells (e.g.: nitride sites, Jahn–Teller Fe^{4+} ions) that trap electrons, hindering carrier mobility, weakening double exchange ferromagnetic interactions and cancelling long range ordering.

^{a} *Institut de Ciència de Materials de Barcelona (ICMAB-CSIC), Campus UAB,
08193 Bellaterra, Spain. E-mail: fontcuberta@icmab.cat,
amparo.fuertes@icmab.es; Fax: +34 935805727; Tel: +34 935801853*

^{b} *Institut Laue-Langevin, 71 Avenue de Martyrs, Grenoble 38000, France*

^{c} *Departament de Geologia, Universitat Autònoma de Barcelona, 08193 Bellaterra,
Spain*

† Electronic supplementary information (ESI) available: Experimental details, and Rietveld refinement information of Sr$_2$FeMoO$_{4.9}$N$_{1.1}$ and Sr$_2$FeMoO$_6$. See DOI: 10.1039/c8cc09845j

SFMO crystallizes in the $I4/m$ space group in a superstructure of the perovskite cubic subcell (of parameter a_p) with unit cell dimensions $\sqrt{2}a_p \times \sqrt{2}a_p \times 2a_p$. Its outstanding physical properties are directly correlated with the mixed electronic states of $Fe^{(2+\delta)+}$ and $Mo^{(6-\delta)+}$ and the degree of order of the two metals in the $2a(0,0,0)$ and $2b(0,0,\frac{1}{2})$ sites respectively.[18] Antisite occupation of Fe/Mo ions typically leads to a reduction of magnetization and of the strength of the double exchange interaction between the magnetic ions.[19,20] On the other hand, it is well known that electron filling of the conducting band in SFMO (mainly of Fe-3d-$t_{2g}\downarrow$–Mo-(4d,5s)$\downarrow$) (Fig. 1a and b) can be modified by appropriate aliovalent doping at A-sites, largely modulating its Curie temperature.[21,22]

In the present work we explore the topotactic introduction of nitride in SFMO. The ultimate goal being the determination of the changes of physical properties in strontium iron molybdenum double perovskite when such substitutions are made at the anionic sublattice, while preserving the chemical ordering of the cationic sublattices. We stress that this approach should, in principle, allow modifying the band filling of Fe–Mo orbitals due to N-promoted cation oxidation, at the cost of perturbing, however, the metal–anion bond network. It will be shown that the obtained oxynitride ($Sr_2FeMoO_{4.9}N_{1.1}$) is ferromagnetic with a relatively high Curie temperature ($T_C \approx 100$ K) which we associate with the presence of a ferromagnetic exchange-like magnetic coupling. However, it is found that the presence of N^{3-} and Fe^{4+} species largely suppresses long-range carrier mobility and limits the extent of spontaneous magnetic ordering, which can be however recovered by application of a magnetic field thus giving rise to a negative magnetoresistance.

The samples have been characterized by chemical analysis, laboratory and synchrotron powder X-ray diffraction, neutron powder diffraction, electron diffraction, Mössbauer spectroscopy, electrical resistivity and magnetisation measurements. Experimental details are provided in the ESI.† SFMO was prepared by treatment in Ar/H_2 (99%/1% v:v) at 1100 °C of a 1:1 mixture of $SrFeO_{3-x}$ and $SrMoO_4$. The oxynitride was stabilized by treatment of 150 mg of SFMO under NH_3 in a narrow range of temperatures and gas flow rates. Ammonolysis during 6 hours at 525–550 °C and 1000 cm³ min⁻¹ leads to samples containing a high proportion, between 40 and 50%, of unreacted SFMO together with the oxynitride. The coexistence of both phases was revealed from high resolution synchrotron powder diffraction data. The analysed nitrogen contents and phase fractions refined by the Rietveld method in several samples were consistent with a constant composition of 1.1 nitrogens per formula in the oxynitride phase. No evidence of the existence of a solid solution $Sr_2FeMoO_{6-x}N_x$ with different N contents was observed. By increasing the temperature the oxynitride fraction is enhanced, and the best sample prepared at 575 °C using the same flow rate and reaction time contained ca. 10% of SFMO. Reactions performed at temperatures above 575 °C or using longer treatment times (i.e. 10 hours) produced cation-disordered samples with the same nitrogen stoichiometry. Totally disordered oxynitride perovskites were obtained by ammonolysis of the mixture of oxides $SrFeO_{3-x}$ and $SrMoO_4$ under similar conditions of temperature and flow rates.

Rietveld refinement of synchrotron X-ray powder diffraction data of the SFMO sample at 90 K in the $I4/m$ space group leads
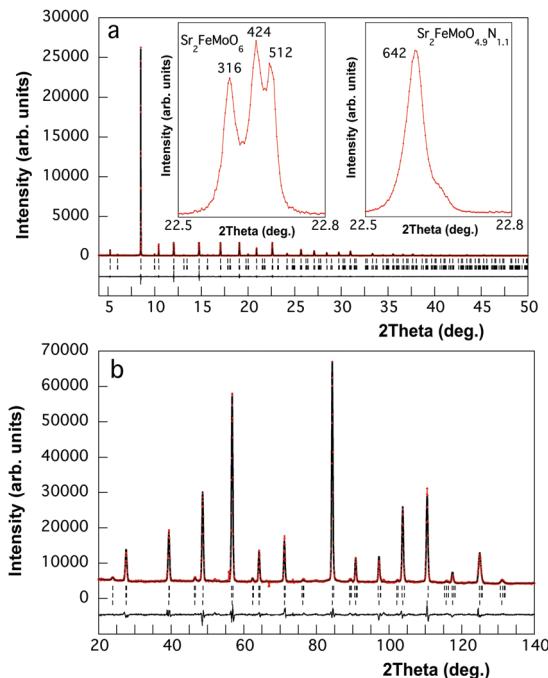
Fig. 2 Rietveld fits to (a) synchrotron X-ray powder diffraction pattern ($\lambda = 0.41269$ Å) and (b) neutron powder diffraction pattern ($\lambda = 1.86502$ Å) of $Sr_2FeMoO_{4.9}N_{1.1}$ at 90 K. In (a) upper and lower ticks mark the reflections of $Fm\bar{3}m$ $Sr_2FeMoO_{4.9}N_{1.1}$ and $I4/m$ SFMO impurity, respectively. In (b) the two upper ticks mark the nuclear and magnetic reflections of SFMO and the lower tick represents the nuclear reflections of $Sr_2FeMoO_{4.9}N_{1.1}$. The insets in (a) show selected regions to illustrate the symmetry change in the oxynitride with respect to the oxide. The small shoulder at the high 2θ side of the 642 reflection corresponds to SFMO (refined fraction: 10.2(2)%).

to cell parameters $a = 5.55568(1)$ and $c = 7.90604(2)$ Å and antisite disorder of 11.2(1)% (see Fig. S1 and Table S1, ESI†). Neutron powder diffraction data at the same temperature showed reflections indicating ferromagnetic order (see Fig. S2 and Table S2, ESI†). The saturation magnetization of this sample at 2 K was 3.3 μ_B per f.u. (see Fig. S3, ESI†) which is consistent with the observed low antisite disorder. The synchrotron X-ray diffraction pattern of $Sr_2FeMoO_{4.9}N_{1.1}$ (Fig. 2a) showed a symmetry increase induced by nitride to cubic $Fm\bar{3}m$ in a unit cell with $a = 2 \times a_p = 7.87774(2)$ Å. The reflection conditions obtained from reconstruction of the reciprocal lattice by electron diffraction were consistent with this space group (see Fig. S4, ESI†). The same space group is shown by the paramagnetic phase of SFMO and reflects the loss of tilting around the c axis present in $I4/m$.

Neutron diffraction patterns have been collected for $Sr_2FeMoO_{4.9}N_{1.1}$ from 1.5 K to 450 K and for Sr_2FeMoO_6 at 90 K.

Ferromagnetic ordering of the oxide secondary phase in the oxynitride sample is reflected in a change in intensity of some diffraction peaks (e.g. 101, Fig. S5, ESI†) for patterns collected below 400 K. A detailed examination of the diffraction data at lower temperatures does not reveal any further enhancement of any other diffraction peak, or the appearance of purely magnetic reflections. In fact, low temperature (1.5 K) neutron data can be satisfactorily refined assuming that the magnetic reflections
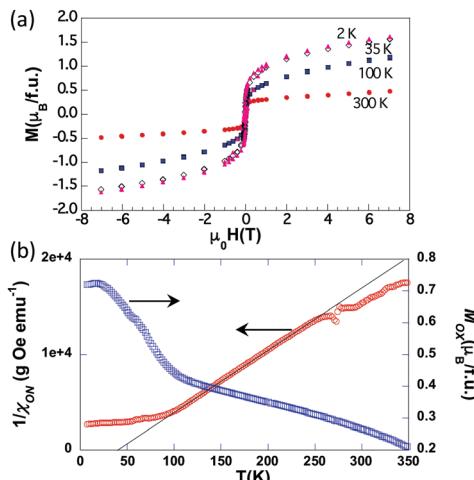
Fig. 3 (a) M–H hysteresis loops of the oxynitride sample; (b) inverse of the magnetic susceptibility of $Sr_2FeMoO_{4.9}N_{1.1}$ (left axis, red symbols), and magnetization assigned to ferromagnetic SFMO (right axis, blue symbols), obtained after the numerical treatment described in the text and detailed in the ESI.†

Table 1 Atomic coordinates in the cubic $Fm\bar{3}m$ space group, cation and anion occupancies and isotropic temperature factors for $Sr_2FeMoO_{4.9}N_{1.1}$ from the refinement to neutron diffraction data at 90 K using $\lambda = 1.86502$ Å[a]

Atom	Wyckoff site	x	y	z	B (Å^2)	Occ. factor
Sr	8c	0.25	0.25	0.25	0.78(3)	1
Fe1/Mo1	4a	0	0	0	0.55(3)	0.825/0.175
Fe2/Mo2	4b	0.5	0.5	0.5	0.87(3)	0.175/0.825
O1/N1	24e	0.2550(3)	0	0	1.11(2)	0.817/0.183

Bond lengths (Å) Sr–O,N ($\times 12$) 2.7853(2), Fe–O,N ($\times 6$) 2.009(2), Mo–O,N ($\times 6$) 1.930(2). [a] Fe/Mo occupation factors were fixed to the refined values from synchrotron diffraction data subject to the ideal stoichiometry (see Table S1, ESI). The N occupation factor was fixed to the analysed stoichiometry. Refined cell parameters were $a = 7.87720(9)$ Å. Agreement factors: $\chi^2 = 4.72$; $R_{wp} = 3.65\%$; and $R_{Bragg} = 2.46\%$.

arise solely from the SFMO phase (ordered moment of Fe $\approx$ 4.3(6) μ_B). This allows us to discard the presence of spontaneous long-range magnetic order beyond a coherence length of a few nanometers. The presence of the ferromagnetic contribution arising from the residual SFMO is clearly visible in the room-temperature $M(H)$ curve shown in Fig. 3(a). Indeed, the measured magnetic moment (≈ 0.3 μ_B per f.u.) is roughly that expected from a 10% fraction of SFMO. Interestingly, the low temperature $M(H)$ magnetization is significantly larger (≈ 1.5 μ_B per f.u.) than expected from this SFMO fraction. In order to explore the magnetic properties of $Sr_2FeMoO_{4.9}N_{1.1}$ we have measured $M(T)$ curves at different applied fields (3, 5, 7, 9 and 11 kOe). We further assume that the total magnetization at every temperature can be expressed as a sum of ferromagnetic and paramagnetic-like contributions: $M(T,H) = M_{OX}(T) + \chi_{ON}(T)\cdot H$. This allows separation of the two contributions to the magnetization: that arise from the FM oxide fraction (M_{OX}), and that from the paramagnetic-like oxynitride ($\chi_{ON}(T)\cdot H$) (further details are given in the ESI†). These two contributions (M_{OX}) and the inverse of the susceptibility (χ_{ON}) are plotted in Fig. 3(b). The inverse susceptibility shows a Curie–Weiss behavior with a positive θ value indicating dominant ferromagnetic interactions within the oxynitride. Below 100 K, obviously $Sr_2FeMoO_{4.9}N_{1.1}$ is no longer a paramagnetic material but its magnetic response gets gradually saturated upon cooling. The enhancement of M_{OX} below this temperature is attributed to a field-induced ferromagnetic contribution of the oxynitride. To rationalize the nature of these magnetic interactions electron counting is compulsory. The substitution of O^{2-} by N^{3-} in Sr_2FeMoO_6 leading to $Sr_2FeMoO_{4.9}N_{1.1}$ induces the oxidation of $Mo^{(6-\delta)+}$ to Mo^{6+} and of $Fe^{(2+\delta)+}$ to $Fe^{(3+x)+}$ ($x \approx 0.1$) as a charge compensation mechanism. The oxidation of (B,B') cations and larger Sr–X (X = anion) bond distance induced by nitride favour the transition from tetragonal to cubic symmetry. The observed tolerance factor calculated as

$t_{obs} = \langle A–X\rangle/\sqrt{2}\langle B–X\rangle$, where $\langle A–X\rangle$ and $\langle B–X\rangle$ are the mean bond distances for A and B sites, respectively, increases from 0.997 in Sr_2FeMoO_6 to 1.000 in $Sr_2FeMoO_{4.9}N_{1.1}$ stabilizing the untilted $Fm\bar{3}m$ structure. The cell volume increases from 243.025(1) Å^3 in SFMO to 244.441(2) Å^3 (normalized to V/2) in $Sr_2FeMoO_{4.9}N_{1.1}$ indicating that the larger ionic radius of nitride outweighs the contraction caused by the oxidation of the cations (see Table 1 and Table S2, ESI†). The presence of Fe ions in an intermediate $Fe^{3.1+}$ valence state can be assessed by Mössbauer spectroscopy. Indeed, the Mössbauer spectrum of the oxynitride can be fitted to the superposition of two contributions, a main component that accounts for 84(2)% of the area and a minor component corresponding to the remaining area (Fig. 4(a)). The isomer shifts (IS), relative to α-Fe, are 0.53(1) and $-0.06(2)$ mm s^{-1}, respectively, which are in the range of expected values for Fe^{3+} and Fe^{4+} ions. The corresponding quadrupolar splittings (of about 0.56(1) and 0.21(2) mm s^{-1}, respectively) show a hierarchy of values typical for Fe^{3+} and Fe^{4+} ions. In this refinement the small contribution (distributed within a large velocity range due to the Zeeman splitting) of the residual SFMO is not included.

The electrical resistivity of the oxynitride sample was measured by using a two contact probe configuration on as-prepared pellets. As shown in Fig. 4(b), the resistivity displays a semiconductor-like behaviour. The concentration of the metallic SFMO residual fraction is well below the 3D percolation limit, this indicates that $Sr_2FeMoO_{4.9}N_{1.1}$ is insulating. In fact, the resistivity data cannot be described by an activated law but by a variable range hopping (VRH) model, suggesting electron motion within localized states. Still a large negative magnetoresistance is measured below 100 K. At first sight, this observation is in contrast to the observed insulating character of the oxynitride. However, a simple and coherent picture can be obtained by noticing that: (a) in the pristine material, the conduction band is populated by minority spin electrons of Fe-3d and Mo-4d,5s parentages, as depicted in Fig. 1a; in a fully ordered SFMO, a periodic arrangement of the regular coordination polyhedra exists and the resulting conduction band is relatively broad and smooth; the ferromagnetic coupling between localized magnetic moments of $3d^5(Fe^{3+})$ core-states is mediated by the free electrons from nominal $Fe^{(2+\delta)+}/Mo^{(6-\delta)+}$ (Fig. 1b); (b) in the oxynitride, N-insertion first oxidizes the metal network, reduces the amount of available electrons and pushes down the Fermi level. As illustrated in Fig. 1c, according to the
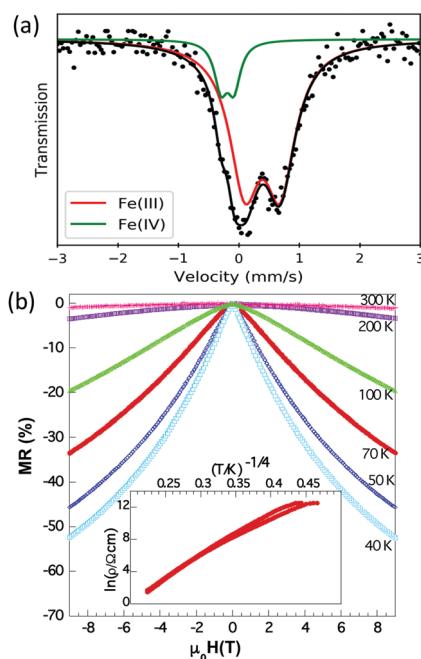
Fig. 4 (a) Mössbauer spectrum of $Sr_2FeMoO_{4.9}N_{1.1}$. The continuous black line is the fit of the spectra using two quadrupolar–split resonant lines as indicated. (b) Magnetoresistance ($M_R = [\rho(H) - \rho(0)]/\rho(0)$) of the oxynitride sample at different temperatures; inset: logarithm of the resistance (at zero field) as a function of $T^{-1/4}$ (variable range hopping behaviour).

electron counting and the Mössbauer results, the Fermi level is placed just under the top of the $3d^{5-x}\uparrow$ spin-up sub-band, anticipating electron itinerancy and establishing a ferromagnetic double exchange coupling between $Fe^{(3+x)+}$ magnetic moments. This is in agreement with $\theta > 0$ observed from magnetic susceptibility data. Next, it breaks the symmetry of the oxygen-bond network and thus introduces a perturbation in the conduction band. Finally, the experimental observation of Fe^{4+} ($3d^4$: t_{2g}^3–e_g^1) ions suggests a potential local deformation of the lattice *via* the Jahn–Teller effect that shall promote the creation of localized states. In Fig. 1d we schematically depict these localized states in the defect-related potential wells. Of course, thermally enhanced electrical conductivity shall occur, which is experimentally observed and consistent with the VRH mechanism identified in the resistivity data. These trapping states imply that formally the double exchange ferromagnetic interaction is locally cancelled and substituted by superexchange antiferromagnetic Fe^{3+}–Fe^{4+} interactions that decouple ferromagnetic patches and, in agreement with neutron data, suppress the long range ferromagnetic order. This magnetic state is reminiscent of a cluster glass. The uncoupled ferromagnetic regions, in the presence of a magnetic field, order along the field direction and an increasingly larger magnetization is observed at $T < 100$ K (Fig. 3a). Most likely, these field oriented regions should promote carrier delocalization and, in agreement with data, a negative magnetoresistance shall be expected, which is in agreement with experimental data. The observation of some hysteresis in the zero-field-cool and field-cool magnetization data (not shown) is also compatible with this scenario.

In conclusion, the double perovskite oxynitride $Sr_2FeMoO_{4.9}N_{1.1}$ with high cation order and cubic $Fm\bar{3}m$ symmetry is obtained by topotactic nitridation of Sr_2FeMoO_6 under NH_3 using high flow rate and moderate temperature conditions. This process, although preserving the cationic order of the oxide, produces dramatic changes in the magnetic structure, mainly related to the lowering of the Fermi level associated with the oxidation of the transition metals induced by nitride, and to carrier localization prompted by disorder induced by the presence of different anions and electron-driven local distortions. These results illustrate the complex interplay of phenomena triggered by nitridation affecting the electronic properties of perovskites.

Conflicts of interest

There are no conflicts to declare.

Notes and references

1 A. Fuertes, *Mater. Horiz.*, 2015, **2**, 453.
2 R. Asahi, T. Morikawa, T. Ohwaki, K. Aoki and Y. Taga, *Science*, 2001, **293**, 269.
3 V. Bachmann, C. Ronda, O. Oeckler, W. Schnick and A. Meijerink, *Chem. Mater.*, 2009, **21**, 316.
4 G. Hitoki, T. Takata, J. N. Kondo, M. Hara, H. Kobayashi and K. Domen, *Chem. Commun.*, 2002, 1698.
5 R. Marchand, *C. R. Acad. Sci.*, 1976, **282**, 329.
6 M. Jansen and H. P. Letschert, *Nature*, 2000, **404**, 980.
7 M. Higashi, R. Abe, T. Takata and K. Domen, *Chem. Mater.*, 2009, **21**, 1543.
8 Y.-I. Kim, P. M. Woodward, K. Z. Baba-Kishi and C. W. Tai, *Chem. Mater.*, 2004, **16**, 1267.
9 A. B. Jorge, J. Oró-Solé, A. M. Bea, N. Mufti, T. T. M. Palstra, J. A. Rodgers, J. P. Attfield and A. Fuertes, *J. Am. Chem. Soc.*, 2008, **130**, 12572.
10 S. Vasala and M. Karppinen, *Prog. Solid State Chem.*, 2015, **43**, 1.
11 A. Fuertes, *Prog. Solid State Chem.*, 2018, **51**, 63.
12 Y.-I. Kim and P. M. Woodward, *J. Solid State Chem.*, 2007, **180**, 3224.
13 C. Pan, T. Takata, M. Nakabayashi, T. Masumoto, N. Shibata, Y. Ikuhara and K. Domen, *Angew. Chem., Int. Ed.*, 2015, **54**, 2955.
14 M. Retuerto, C. de la Calle, M. J. Martínez-Lope, F. Porcher, K. Krezhov, N. Menéndez and J. A. Alonso, *J. Solid State Chem.*, 2012, **185**, 18.
15 R. Ceravola, J. Oró-Solé, A. P. Black, C. Ritter, I. Puente Orench, I. Mata, E. Molins, C. Frontera and A. Fuertes, *Dalton Trans.*, 2017, **46**, 5128.
16 K. L-Kobayashi, T. Kimura, H. Sawada, K. Terakura and Y. Tokura, *Nature*, 1998, **395**, 677.
17 D. Serrate, J. M. De Teresa and M. R. Ibarra, *J. Phys.: Condens. Matter*, 2007, **9**, 023201.
18 Y. H. Huang, M. Karppinen, H. Yamahuchi and J. B. Goodenough, *Phys. Rev. B: Condens. Matter Mater. Phys.*, 2006, **73**, 104408.
19 J. Navarro, J. Nogués, J. S. Muñoz and J. Fontcuberta, *Phys. Rev. B: Condens. Matter Mater. Phys.*, 2003, **67**, 174416.
20 C. Frontera and J. Fontcuberta, *Phys. Rev. B: Condens. Matter Mater. Phys.*, 2004, **69**, 014406.
21 D. Rubi, C. Frontera, J. Fontcuberta, M. Wojcik, E. Jedryka and C. Ritter, *Phys. Rev. B: Condens. Matter Mater. Phys.*, 2004, **70**, 094405.
22 D. Rubi, C. Frontera, J. Nogués and J. Fontcuberta, *J. Phys.: Condens. Matter*, 2004, **16**, 3173.